ELSEVIER

www.elsevier.nl/locate/jorganchem

Journal of Organometallic Chemistry 611 (2000) 164–171

Journal of Organometallic Chemistry

Structural characteristics of areneselenenyl bromide and areneselenenyl chloride stabilized by hypervalent coordination with a halide anion in the solid state

Michio Iwaoka, Hiroto Komatsu, Shuji Tomoda *

Department of Life Sciences, Graduate School of Arts and Sciences, The University of Tokyo, Komaba, Meguro-ku, Tokyo 153-8902, Japan

Received 28 February 2000; accepted 30 March 2000

Abstract

Solid-state molecular structures of 2-[(*N*-cyclohexyl-*N*-methylamino)methyl]benzeneselenenyl bromide (ArSeBr) and chloride (ArSeCl), stabilized by hypervalent coordination with a halide anion (Br^- or Cl^-, respectively), were determined by X-ray diffraction method. By comparing bond parameters of the observed hypervalent Br–Se···Br fragment with those reported previously for other organoselenium compounds, which have a similar T-shaped selenium fragment, it was revealed that there is decent hyperbolic relationship between the two linear Se–Br atomic distances in the solid state, reflecting the possibility of a pathway for the addition reaction of benzeneselenenyl bromide (PhSeBr) in solution. In addition, the existence of significant bond-shortening (~ 0.1 Å) due to intermolecular weak packing interactions was strongly suggested by comparison of the extrapolated Se–Br covalent bond length (2.220 Å) in the solid state with that reported for PhSeBr (2.325 Å) in the gas phase. Ab initio molecular orbital calculations at the RHF/6-31G(d,p) level using Ahlrichs pVDZ basis sets for Se and Br estimated the perturbation energy in the solid state to be roughly 1.5 kcal mol^{-1} independent of the packing structure.

Keywords: Areneselenenyl bromide; Areneselenenyl chloride; Hypervalent interaction; Structural correlation; Packing force

1. Introduction

Determination of molecular structures in the solid state is a valuable experimental strategy to understand chemical properties of organic compounds as well as to deduce structural transformation along the reaction pathways [1]. Recently, Landrum and Hoffmann [2] reported comprehensive search of the Cambridge Structural Database (CSD) [3] for linear X–Q–X fragments, where X is a halogen and Q is a chalcogen (Group 16) or pnicogen (Group 15) element. They found two types of structural correlations between the two Q–X atomic distances, one of which (the hyperbolic correlation) appears to represent the addition reaction pathway of X to a Q–X bond. Similar structural correlations have been discussed frequently in the literature [1,4].

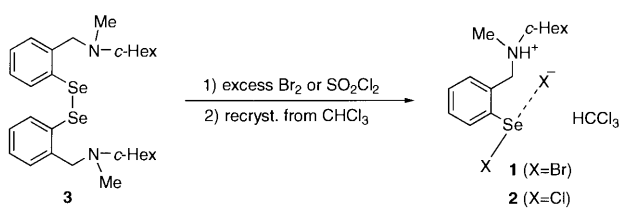

Scheme 1.

Benzeneselenenyl halides (PhSeX, X = Br and Cl) are useful electrophilic selenium reagents in organic synthesis [5]. However, the structural information is limited because they are usually highly reactive. Most of selenenyl bromides, the molecular structures of which have been determined in the gas phase or in the solid state, were significantly stabilized by hypervalent coordination with an intra- or intermolecular nucleophile [6]. To obtain the structure free from such coordination, the molecular structure of benzeneselenenyl bromide (PhSeBr) has been determined by electron diffraction method: the reported Se–Br covalent bond length in the

* Corresponding author. Fax: +81-3-54546998.
E-mail address: tomoda@selen.c.u-tokyo.ac.jp (S. Tomoda).

0022-328X/00/$ - see front matter
PII: S0022-328X(00)00434-4

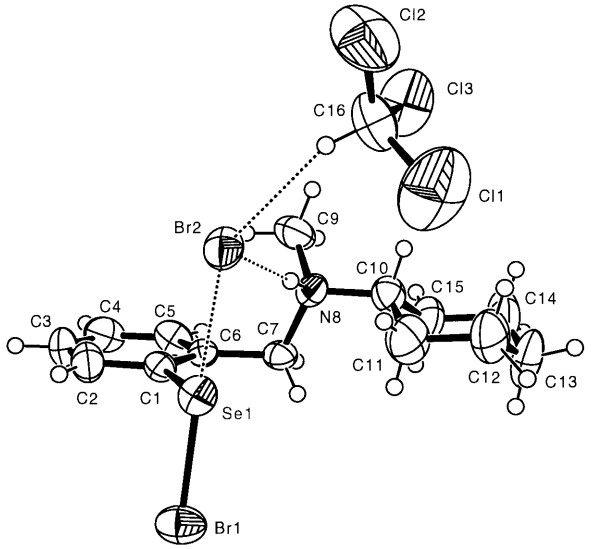

Fig. 1. ORTEP plot for **1** at the 50% probability level.

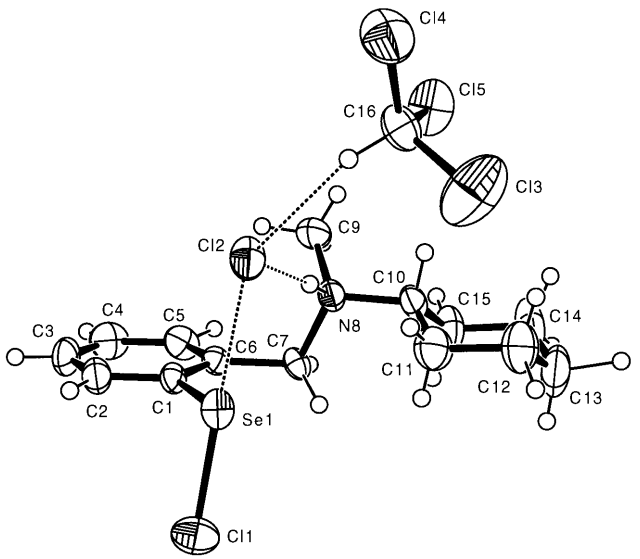

Fig. 2. ORTEP plot for **2** at the 50% probability level.

isolated state was 2.325(2) Å [7]. On the other hand, rather rare structural data are available for selenenyl chlorides [8]. Consequently, pathways for the electrophilic addition reactions of PhSeBr and PhSeCl have not been thoroughly understood due to the lack of sufficient structural data.

In the course of our recent research on nonbonded weak inter-element interactions involving a divalent organic selenium [9], we obtained single crystals of areneselenenyl bromide **1** and chloride **2**, which are significantly stabilized by hypervalent coordination with the corresponding halide anions (Br^- and Cl^-, respectively). In this paper, molecular structures of these unique T-shaped selenium compounds have been determined by X-ray analysis, and bond parameters of the linear Br–Se···Br and Cl–Se···Cl fragments observed for **1** and **2**, respectively, have been compared with those reported previously in the literature [10–16]. Remarkable hyperbolic relationship was found for the Br–Se···Br fragment, whereas for the Cl–Se···Cl fragment the structural data were too few to deduce such relationship. It is proposed herein that the observed hyperbolic relationship is useful for understanding pathways for the addition reactions of PhSeX in solution as well as for estimating the perturbation energy in the solid state arising from weak intermolecular interactions.

2. Results and discussion

2.1. Synthesis of *1* and *2*

Compounds **1** and **2** were synthesized according to Scheme 1. Treatment of diselenide **3** (ArSeSeAr) [9a], which has intramolecular tertiary amino groups, with an excess amount of bromine in carbon tetrachloride gave the crude product [17]. This was then recrystallized from chloroform to obtain **1** in 63% yield as fine red–brown crystals. Similarly, **2** was obtained in 28% yield as fine yellow crystals by using sulfuryl chloride (SO_2Cl_2) instead of bromine. The mechanisms of these reactions are not yet clear, but it is plausible that the corresponding selenenyl trihalides ($ArSeX_3$) [18] might intervene in the formation of **1** and **2**. Molecular structures of these complexes were determined by X-ray analysis and were confirmed by elemental analysis.

2.2. X-ray analysis of *1* and *2*

Molecular structures of **1** and **2** determined by X-ray analysis are shown in Figs. 1 and 2, respectively. It is seen clearly that both compounds possess almost identical molecular structure with each other in the solid state, except that two bromine atoms (Br1 and Br2) of **1** are substituted with two chlorine atoms (Cl1 and Cl2) for **2**.

The structure of each compound consists of three segments. The largest segment is areneselenenyl bromide (ArSeBr) or chloride (ArSeCl). This has a protonated intramolecular tertiary amino group, carrying a unit positive charge. The ammonium protons were found by Fourier synthesis after the least-squares fitting of the locations and anisotropic parameters for all non-hydrogen atoms. The second segment is the counter anion (Br^- or Cl^-) located at the backside of the Se–Br or Se–Cl bond of the first segment. There is significant close contact between the counter halide anion and the divalent selenium atom (Se1···Br2 = 2.769 for **1**, Se1···Cl2 = 2.676 Å for **2**), forming a T-shaped coordinate structure around the selenium.

Detailed structural characteristics of the T-shaped selenium are discussed in the subsequent sections. There is another inter-segment interaction, i.e. an N–H···Br^- or N–H···Cl^- hydrogen bond, between the ammonium nitrogen of the first segment and the halide anion (N8···Br2 = 3.279 for **1**, N8···Cl2 = 3.105 Å for **2**). The third segment is a chloroform molecule, which has a weak interaction with the halide anion through C–H···Br^- or C–H···Cl^- hydrogen bond (C16···Br2 = 3.72 for **1**, C16···Cl2 = 3.577 Å for **2**). Selected intra- and inter-segment bond parameters for **1** and **2** are listed in Tables 1 and 2, respectively. It should be noted that these bond parameters could be significantly different from those expected for similar compounds in the gas phase (or in the solution) due to the presence of intermolecular weak packing interactions in the solid state.

Table 1
Selected bond parameters (atomic distances (Å), angles (°), torsion angles (°)) for **1** in the solid state

Se1–Br1	2.474(2)
Se1–C1	1.944(9)
Se1···Br2	2.769(2)
N8···Br2	3.279(8)
C16···Br2	3.72(1)
H(N8)···Br2	2.34
H(C16)···Br2	2.84
Br1–Se1–C1	91.5(3)
Br1–Se1···Br2	177.43(6)
C1–Se1···Br2	88.7(3)
Se1···Br2···N8	74.0(1)
Se1···Br2···C16	138.9(2)
N8···Br2···C16	95.5(2)
N8–H···Br2	173
C16–H···Br2	154
Br1–Se1–C1–C2	83.6(7)
Br1–Se1–C1–C6	−95.0(7)
Br2···Se1–C1–C2	−99.0(7)
Br2···Se1–C1–C6	82.4(7)

Table 2
Selected bond parameters (atomic distances (Å), angles (°), torsion angles (°)) for **2** in the solid state

Se1–Cl1	2.307(2)
Se1–C1	1.919(5)
Se1···Cl2	2.676(2)
N8···Cl2	3.105(5)
C16···Cl2	3.577(6)
H(N8)···Cl2	2.12
H(C16)···Cl2	2.63
Cl1–Se1–C1	91.6(1)
Cl1–Se1···Cl2	177.30(5)
C1–Se1···Cl2	86.9(1)
Se1···Cl2···N8	78.07(8)
Se1···Cl2···C16	139.5(1)
N8···Cl2···C16	94.5(1)
N8–H···Cl2	174
C16–H···Cl2	156
Cl1–Se1–C1–C2	79.6(4)
Cl1–Se1–C1–C6	−99.6(4)
Cl2···Se1–C1–C2	−102.6(4)
Cl2···Se1–C1–C6	78.2(4)

2.3. Structural characteristics of the X–Se···X fragments of **1** and **2**

The Br–Se···Br fragment of **1** was approximately linear (Br1–Se1···Br2 177.43°) and perpendicular to the Se–C bond (Br1–Se1–C1 91.5, C1–Se1···Br2 88.7°). Thus, the selenium center formed an almost complete T-shaped trivalent coordinate in the solid state. However, the two Se–Br atomic distances were significantly different from each other (Se–Br = 2.474 and 2.769 Å, $\Delta_{Se-Br} = 0.295$ Å). The bond length discrepancy may be mainly due to the two hydrogen bonds to the bromide anion (Br2), which should significantly reduce the nucleophilicity of Br2. The dihedral angle between the linear Br–Se···Br fragment and the benzene plane was 83° on the average, allowing an efficient orbital overlap between the weak Se–Br bonds and the aromatic π orbitals.

Comparison of the above structural features with those reported for PhSeBr in the gas phase [7] may be useful for understanding the reaction pathway of PhSeBr. The bond parameters of PhSeBr in the gas phase are 2.325(2) Å for the Se–Br covalent bond length, 1.899(6) Å for the Se–C bond length, 99.8(1.2)° for the Br–Se–C bond angle, and 68.4(2.4)° for the dihedral angle between the Se–Br bond and the benzene plane [7]. The significant bond elongation (0.149 Å) for the Se1–Br1 bond of **1** compared to PhSeBr is reasonably explained by the presence of strong coordination of the bromide anion (Br2) to the selenium atom (Se1), suggesting that the observed T-shaped structure can be a good model for the transient structure on the reaction pathway for $PhSeBr + Br^- \rightarrow PhSeBr_2^-$. The approximately perpendicular dihedral angle between the Br–Se···Br fragment and the benzene plane observed for **1** also supports the resemblance to the transient structure along the addition reaction pathway, which is deducible from the gas-phase molecular structure of PhSeBr.

A similar T-shaped structure involving a linear Cl–Se···Cl fragment was observed for **2**. The angles around the trivalent selenium center were 177.30° (Cl1–Se1···Cl2), 91.6° (Cl1–Se1–C1), and 86.9° (C1–Se1···Cl2), which are almost identical with those observed for **1**. However, distortion of the two Se–Cl atomic distances for **2** (Se–Cl = 2.307 and 2.676 Å, $\Delta_{Se-Cl} = 0.369$ Å) seemed to be more pronounced than that observed for **1** ($\Delta_{Se-Br} = 0.295$ Å), suggesting that the electrophilicity of PhSeBr is slightly higher than that of PhSeCl. The dihedral angle between the linear

Table 3
Results of CSD and literature surveys for linear Br–Se···Br and Cl–Se···Cl fragments of T-shaped trivalent organic selenium compounds

Compound	d_1 (Å)	d_2 (Å)	CSD refcode	Reference
$Br\overset{d_1}{-}Se\overset{d_2}{\cdots}Br$				
$[(CH_3)C_3N_2H_2(SeBr_2)–CH_2–]_2$	2.521	2.662		[10]
	2.531	2.650		
p-$C_6H_4(SeBr)_2$	2.311	3.684	RAGROG	[11]
$[4\text{-}(BrSe)C_6H_4]_2SeBr_2$	2.337	3.184	RAGRUM	[11]
$(C_5H_5N)CH_2CH_2SeBr_2$	2.499	2.687	YERHUY	[12]
$(C_9H_7N)CH_2CH_2SeBr_2$	2.541	2.641	ZADNOH	[12]
$3\text{-}Br(C_5H_4N)CH_2CH_2SeBr_2$	2.463	2.767	ZADNEX	[12]
$4\text{-}(CN)(C_5H_4N)CH_2CH_2SeBr_2$	2.480	2.718	ZADNIB	[12]
$[C_6H_5(CH_3)_3N]SeBr_2CN$	2.530	2.624	PEBPOB	[13]
$[(CH_3)_4N]SeBr_2CN$	2.575	2.575		[14]
$[(BEDT–TTF)_2]SeBr_2CN$	2.564	2.586	YEMCU001	[15]
$(Se_3C)SeBr_2$	2.508	2.619	CIFZUM	[16]
1	2.474	2.769		This work
$Cl\overset{d_1}{-}Se\overset{d_2}{\cdots}Cl$				
$[(CH_3)_4N]SeCl_2CN$	2.425	2.425		[14]
2	2.307	2.676		This work

Cl–Se···Cl fragment and the benzene plane was 79° on the average, which is slightly smaller than that observed for **1**. These structural characteristics of the Cl–Se···Cl fragment observed for **2** could not be compared with the molecular structure of PhSeCl in the absence of experimental data.

2.4. Database analysis of linear X–Se···X fragments

In order to elucidate more clearly the structural characteristics of the linear X–Se···X (X = Br and Cl) fragments observed for **1** and **2**, similar X–Se···X fragments were surveyed in the literature. Since our interest focused on the reaction pathways of PhSeBr and PhSeCl in solution, we carried out database search under restricted conditions, i.e. only for linear Br–Se···Br and Cl–Se···Cl fragments of T-shaped organic selenium compounds. The results are summarized in Table 3. Comprehensive search for the same fragments in CSD without the restrictions has been reported recently by Landrum and Hoffmann [2].

Nine linear Br–Se···Br fragments were hit in CSD [3] and three more analogous fragments were found independently by the literature survey under our criteria noted above. Among these 12 fragments, four possessed an aromatic substituent at the central Se atom like compound **1**, four possessed an alkyl substituent, and three possessed a cyano substituent. The other one was a miscellaneous case.

Structural correlation between the two Se–Br atomic distances (d_1 and d_2) of the 12 Br–Se···Br fragments obtained (open circles) and that observed for **1** (filled circles) is shown in Fig. 3. The plots are symmetrically expanded to show excellent hyperbolic correlation between d_1 and d_2 [19]. It may be reasonable to assume that this correlation should reflect the pathway for the addition reaction between PhSeBr and Br^- in solution, even although intermolecular packing forces do not exist in the solution. Clustering of the structural data in the range of 2.46 Å $< d_1$ (and d_2) $<$ 2.77 Å is consistent with the anticipation that the stable reaction adduct should have symmetrical structure ($d_1 = d_2$). It is worth noting that only marginal substitution effect on the magnitude of d_1 and d_2 was observed in the hyperbolic relationship in spite of the substituent variation at the

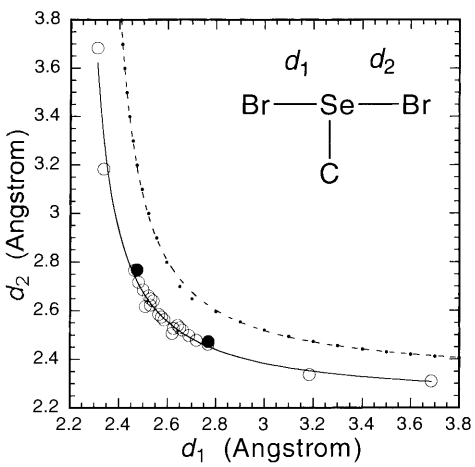

Fig. 3. Correlation plots between the two Se–Br atomic distances (d_1 and d_2) of a linear Br–Se–Br fragment involving a T-shaped organic selenium. Open circles represent the structures of 12 Br–Se–Br fragments found in the literature, and filled circles represent the structure of **1**. Dots represent the calculated structures along the optimal pathway for $PhSeBr + Br^- \rightarrow PhSeBr_2^-$ in vacuo at the RHF/6-31G(d,p) level using Ahlrichs pVDZ basis sets for Se and Br. The solid and dashed curves are depicted by using the parameters obtained from the hyperbolic data fitting (see text for details).

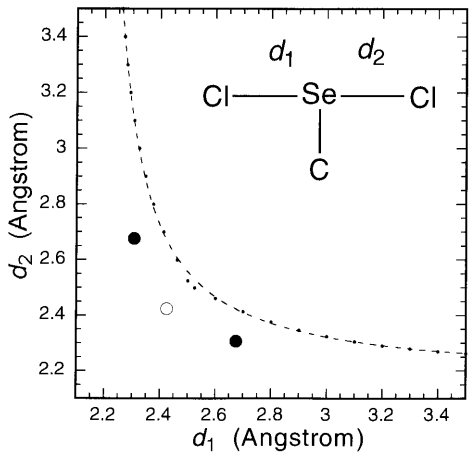

Fig. 4. Correlation plots between the two Se–Cl atomic distances (d_1 and d_2) of a linear Cl–Se–Cl fragment involving a T-shaped organic selenium. An open circle represents the structure of a symmetrical Cl–Se–Cl fragment found in the literature, and filled circles represent the structure of **2**. Dots represent the calculated structures along the optimal pathway for $PhSeCl + Cl^- \rightarrow PhSeCl_2^-$ in vacuo at the RHF/6-31G(d,p) level using Ahlrichs pVDZ basis sets for Se. The dashed curves is depicted by using the parameters obtained from the hyperbolic data fitting (see text for details).

selenium atom for a total of 13 Br–Se···Br fragments including **1**.

Fitting the data to the hyperbolic equation, $(d_1 - D_s)(d_2 - D_s) = C$, where D_s represents the extrapolated Se–Br covalent bond length for PhSeBr in the solid state and C is a constant, yielded the values of 2.220 ± 0.005 (Å) and 0.127 ± 0.006 (Å^2) for D_s and C, respectively, with a high correlation coefficient ($r^2 = 0.984$). The fitting curve is drawn with solid line in Fig. 3. The converged ultimate value of the Se–Br bond length (D_s) was found to be shorter by 0.103 Å than the experimental Se–Br bond length of PhSeBr in the gas phase ($D_g = 2.325$ Å) [7].

On the other hand, only one fragment was found in the literature as for the Cl–Se···Cl fragment. The fragment possessed a cyano substituent at the Se atom, and the structure was crystallographically C_{2v} symmetric. Fig. 4 shows the structural correlation between the two Se–Cl atomic distances observed for the symmetrical compound (an open circle) and **2** (filled circles). Since the number of the structural data was too few at present, hyperbolic structural correlation could not be assumed for the Cl–Se···Cl fragment in the solid state.

2.5. Bond-shortening effect in the solid state

Comparison of the Se–Br covalent bond length in the solid state ($D_s = 2.220$ Å), which was extrapolated by the data fitting, with the one in the gas phase (PhSeBr; $D_g = 2.325$ Å) [7], revealed the existence of significant bond shortening (0.103 Å) in the solid state. The origin of this bond-shortening effect is most probably ascribed to intermolecular packing forces in the solid state. Therefore, the observed remarkable hyperbolic relationship may imply that the net perturbation energies due to solid-state weak packing interactions remain constant within the series of the totally 13 Br–Se···Br fragments including **1**, although each fragment may exhibit different packing pattern in the solid state.

In order to estimate the net perturbation energy in the solid state, ab initio molecular orbital calculations [20] of the nucleophilic addition reaction pathway ($PhSeBr + Br^- \rightarrow PhSeBr_2^-$) in vacuo were performed at the RHF/6-31G(d,p) level using Ahlrichs pVDZ basis sets [21] for Se and Br. The optimized structures with one of the Se–Br atomic distances frozen at 2.7–3.8 Å with 0.1 Å interval are shown in Fig. 3 with dots, and the hyperbolic fitting curve $[(d_1 - D_{fit})(d_2 - D_{fit}) = C, D_{fit} = 2.310 \pm 0.001$ Å, $C = 0.143 \pm 0.002$ Å^2] is drawn with dashed line. The fitting result was excellent ($r^2 = 0.999$). Furthermore, the extrapolated Se–Br covalent bond length in vacuo (2.310 Å) was in good agreement with that of PhSeBr determined experimentally in the gas phase (2.325 Å) [7] as well as that calculated directly for PhSeBr in vacuo (2.349 Å) at the same level, suggesting structural accuracy of the calculations.

It is seen clearly in Fig. 3 that the structure of the Br–Se···Br fragment shrinks to a significant extent in the solid state compared to the isolated state in vacuo. This shrinking may not be due to calculation errors at the RHF level not only because the experimentally determined Se–Br bond length of PhSeBr was well reproduced by the calculations as described above but also because including electron correlation in the calculations tended to exaggerate the structural discrepancy between in the solid state and in vacuo. For example, the density functional calculations (B3LYP) [22] enlarged the discrepancy by 0.012 Å for the symmetrical stable adduct.

Provided that the observed discrepancy between the solid-state structural correlation for the Br–Se···Br fragment and the reaction pathway calculated for $PhSeBr + Br^- \rightarrow PhSeBr_2^-$ in vacuo can be ascribed to the presence of intermolecular weak packing forces in the solid state, the perturbation energy due to the packing interactions can be roughly estimated by energy calculations along both hyperbolic curves in Fig. 3. The potential energy profiles are shown in Fig. 5. The minimum energy for the structural correlation in the solid state ($d_1 = d_2 = 2.575$ Å) was found to be 1.52 kcal mol^{-1} less stable than that for the calculated optimal reaction pathway ($d_1 = d_2 = 2.669$ Å). Thus, the solid-state perturbation energy was roughly estimated to be about 1.5 kcal mol^{-1} for the Br–Se···Br fragment. Parallelism of the two energetic curves in Fig. 5 strongly suggested that the perturbation energy may be approximately constant for all Br–Se···Br fragments in the solid state, although each fragment is involved in different packing pattern.

For the Cl–Se···Cl fragment, the reaction pathway for $PhSeCl + Cl^- \rightarrow PhSeCl_2^-$ calculated in vacuo is shown in Fig. 4 with dots, and the fitting curve [$(d_1 - D_{fit})(d_2 - D_{fit}) = C$, $D_{fit} = 2.164 \pm 0.002$ Å, $C = 0.132 \pm 0.003$ Å^2, $r^2 = 0.999$] is drawn with dashed line. Comparing the calculated pathway with the structures determined in the solid state, it may be possible to assume the presence of a bond-shortening effect in the solid state similarly to the case of the Br–Se···Br fragment.

3. Conclusions

It was revealed that the molecular structures of **1** and **2** in the solid state possess T-shaped coordination structure around the selenium with a linear X–Se···X (X = Br or Cl, respectively) fragment. By comparing bond parameters of the observed X–Se···X fragments with those reported previously for other organoselenium compounds, which have a similar T-shaped selenium, in the solid state and PhSeBr in the gas phase, four structural characteristics of the X–Se···X fragments in the solid state are noteworthy: (1) decent hyperbolic relationship between the two linear Se–Br atomic distances exists for the Br–Se···Br fragment in the solid state, reflecting the addition reaction pathway for $PhSeBr + Br^- \rightarrow PhSeBr_2^-$ in solution; (2) the Br–Se···Br fragment in the solid state may possibly shrink by ~ 0.1 Å, compared to that expected in the gas phase, due probably to the presence of intermolecular weak packing interactions in the solid state; (3) magnitude of the solid-state perturbation energy (~ 1.5 kcal mol^{-1}) around the Br–Se···Br fragment would be independent of the packing structure; and (4) similar considerations may be applied for the Cl–Se···Cl fragment. Although the mechanism of the bond-shortening effect in the solid state is not clear at present, it should be pointed out that the relatively weak inter-element hypervalent bonding can be a useful probe to estimate intermolecular packing forces in the solid state.

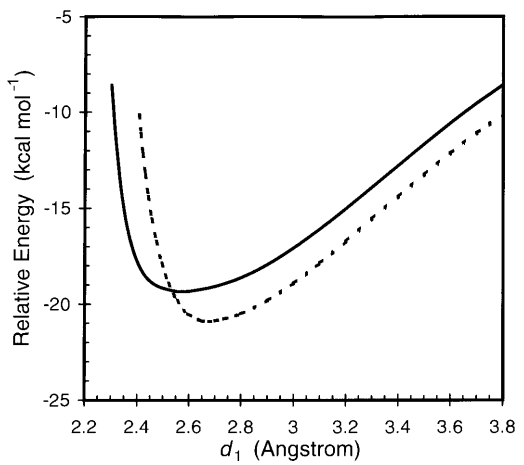

Fig. 5. Potential profiles calculated at the RHF/6-31G(d,p) level using Ahlrichs pVDZ basis sets for Se and Br. Relative energies are with respect to the separated state ($PhSeBr + Br^-$). The solid curve is drawn along the structural correlation observed for the linear Br–Se···Br fragments in the solid state. The dashed curve is drawn along the reaction pathway calculated for $PhSeBr + Br^- \rightarrow PhSeBr_2^-$ in vacuo.

4. Experimental

4.1. Synthesis of N-cyclohexyl-N-methyl-o-(bromoseleno)benzylammonium bromide (1)

Under a continuous flow of dry gaseous nitrogen, diselenide **3** [9a] (56.3 mg, 0.1 mmol) was dissolved in 5 ml of dry carbon tetrachloride (CCl_4), and the solution was added with 5 ml (0.15 mmol) of 0.03 M bromine solution in CCl_4. The resulting red–yellow suspension was stirred for 30 min at room temperature. After removal of the solvent in vacuo, red–brown viscous material was obtained, which was then recrystallized from chloroform. Compound **1** was obtained as fine red–brown crystals in 64% yield (45.8 mg). Anal. Calc. for $C_{15}H_{22}Br_2Cl_3NSe$: C, 32.09; H, 3.95; N, 2.49. Found: C, 31.97; H, 3.90; N, 2.63%.

4.2. X-ray crystal structure analysis of 1

A Rigaku AFC6S diffractometer was employed with the Mo–K_α ($\lambda = 0.71073$ Å) radiation monochromatized by graphite. Intensity data were collected using an ω–2θ scan technique to a maximum 2θ value of 50.0°. A total of 3898 reflections was collected. The structure was solved by the direct method (SIR-92) [23]. The final full-matrix least-squares refinement of F^2 against all unique 3860 reflections ($R_{int} = 0.054$) was performed by using the SHELXL-97 program [24]. The crystal data obtained are as follows: formula, $C_{14}H_{21}BrNSe \cdot Br \cdot CHCl_3$; M, 561.47; space group, monoclinic $P2_1/a$ (no. 14); a, 10.467(1); b, 16.164(2); c, 12.412(1) Å; β, 96.50(1)°; V, 2086.5(4) Å^3; Z, 4; μ, 6.0 mm^{-1}; D_{calc}, 1.787 g ml^{-1}; T, 296 K; size, $0.20 \times 0.20 \times 0.20$ mm; number of variables, 220; $R(F^2)$, 0.061; $wR(F^2)$, 0.148. The graphical molecular structure of **1** (Fig. 1) was drawn using the ORTEP-3 program for Windows [25].

4.3. Synthesis of N-cyclohexyl-N-methyl-o-(chloroseleno)benzylammonium chloride (2)

Under a continuous flow of dry gaseous nitrogen, diselenide **3** [9a] (56.3 mg, 0.1 mmol) was dissolved in 5 ml of dry CCl_4, and the solution was added with 5 ml (0.15 mmol) of 0.03 M sulfuryl chloride (SO_2Cl_2) solu-

tion in CCl_4. The resulting yellow suspension was stirred for 30 min at room temperature. After removal of the solvent in vacuo, yellow crystals were obtained, which were then recrystallized from chloroform. Compound **2** was obtained as fine yellow crystals in 28% yield (17.5 mg). Anal. Calc. for $C_{15}H_{22}Cl_5NSe$: C, 38.12; H, 4.69; N, 2.96. Found: C, 38.03; H, 4.61; N, 2.98%.

4.4. X-ray crystal structure analysis of **2**

A Rigaku AFC6S diffractometer was employed with the Cu–K_α ($\lambda = 1.54184$ Å) radiation monochromatized by graphite. Intensity data were collected using an ω–2θ scan technique to a maximum 2θ value of 120.0°. A total of 3052 reflections was collected. The structure was solved by the direct method (SIR-92) [23]. The final full-matrix least-squares refinement of F^2 against all unique 2877 reflections ($R_{int} = 0.099$) was performed by using the SHELXL-97 program [24]. The crystal data obtained are as follows: formula, $C_{14}H_{21}ClNSe\cdot Cl\cdot CHCl_3$; M, 472.55; space group, monoclinic $P2_1/a$ (no. 14); a, 10.426(2); b, 16.010(3); c, 12.005(1) Å; β, 95.37(1)°; V, 1995.1(6) Å^3; Z, 4; μ, 8.7 mm^{-1}; D_{calc}, 1.573 g ml^{-1}; T, 296 K; size, $0.30 \times 0.20 \times 0.20$ mm; number of variables, 287; $R(F^2)$, 0.063; $wR(F^2)$, 0.148. The graphical molecular structure of **2** (Fig. 2) was drawn using the ORTEP-3 program for Windows [25].

4.5. Data analysis

Cambridge Structural Database (CSD) [3] system version 5.16 (released in 1999) was used for the search of Br–Se···Br and Cl–Se···Cl fragments in the solid state. The restricted conditions, i.e., only for linear Br–Se···Br and Cl–Se···Cl fragments of T-shaped organic selenium compounds, were applied. The results are given in Table 3.

For fitting the structural data to a hyperbolic equation, KaleidaGraph version 3.08 (Synergy Software, Reading, PA) was used, in which the Levenberg-Marquardt algorithm [26] was employed for the non-linear least-squares method.

4.6. Molecular orbital calculations

All ab initio molecular orbital calculations were carried out by using GAUSSIAN-94 program [20]. For calculating the nucleophilic addition reaction pathway for $PhSeBr + Br^- \rightarrow PhSeBr_2^-$ in vacuo, the structure was optimized fully at the RHF/6-31G(d,p) level using Ahlrichs pVDZ basis sets [21] for Se and Br with one of the Se–Br atomic distances (for example, d_1) frozen at 2.7–3.8 Å with an interval of 0.1 Å. Similarly, the reaction pathway for $PhSeCl + Cl^- \rightarrow PhSeCl_2^-$ in vacuo was calculated by fully optimizing the structure at the same level with one of the Se–Cl atomic distances frozen at 2.5–3.5 with 0.1 Å interval.

The energetic profile along the reaction pathway for $PhSeBr + Br^- \rightarrow PhSeBr_2^-$ (a dashed curve in Fig. 5) was directly obtained from the above calculations. On the other hand, the energetic profile along the structural correlation observed in the solid state (a solid curve in Fig. 5) was obtained by fixing both Se–Br atomic distances (d_1 and d_2) at the calculated distances from the hyperbolic equation, $(d_1 - 2.220)(d_2 - 2.220) = 0.127$. The other structural parameters were optimized fully at the RHF/6-31G(d,p) level using Ahlrichs pVDZ basis sets [21] for Se and Br. The obtained relative energies with respect to the separated state ($PhSeBr + Br^-$) were not corrected with the basis set superposition errors (BSSE).

5. Supplementary material

Crystallographic data for the structural analysis has been deposited with the Cambridge Crystallographic Data Centre, CCDC nos. 140830 and 140831. Copies of this information may be obtained free of charge from: The Director, CCDC, 12 Union Road, Cambridge, CB2 1EZ, UK (fax: +44-1223-336033; e-mail: deposit@ccdc.cam.ac.uk or www: http://www.ccdc.cam.ac.uk).

Acknowledgements

We thank Professor K. Ogawa and Dr J. Harada for experimental supports in the X-ray analysis. This work was supported by the Grants-in-Aid for Scientific Research nos. 11120210 and 10133207 from the Ministry of Education, Science, Sports and Culture, Japan.

References

[1] (a) H.B. Bürgi, J.D. Dunitz, Acc. Chem. Res. 16 (1983) 153. (b) H.B. Bürgi, J.D. Dunitz (Eds.), Structure Correlation, vols. 1 and 2, VCH, Weinheim, 1994.
[2] G.A. Landrum, R. Hoffmann, Angew. Chem. Int. Ed. Engl. 37 (1998) 1887.
[3] F.H. Allen, J.E. Davies, O.J. Johnson, O. Kennard, C.F. Macrae, E.M. Mitchell, G.F. Smith, D. Watson, J. Chem. Inf. Comput. Sci. 31 (1991) 187.
[4] (a) H.B. Bürgi, Angew. Chem. Int. Ed. Engl. 14 (1975) 460. (b) H.B. Bürgi, Inorg. Chem. 12 (1973) 2321. (c) D. Britton, J.D. Dunitz, J. Am. Chem. Soc. 103 (1981) 2971. (d) W. Clegg, R.J. Errington, G.A. Fisher, D.C.R. Hockless, N.C. Norman, A.G. Orpen, S.E. Stratford, J. Chem. Soc. Dalton Trans. (1992) 1967.
[5] M. Iwaoka, S. Tomoda, in: L.A. Paquette (Ed.), Encyclopedia of Reagents for Organic Synthesis, Wiley, Chichester, 1995.
[6] (a) N.M. Zaripov, A.V. Golubinskii, S.V. Sokolkov, L.V. Vilkov, T.G. Mannafov, Dokl. Akad. Nauk SSSR 278 (1984) 664. (b) P.M. Baiwir, G. Llabrés, O. Dideberg, L. Dupont, J.L.

Piette, Acta Crystallogr. Sect. B 31 (1975) 2188. (c) R. Kaur, H.B. Singh, R.P. Patel, J. Chem. Soc. Dalton Trans. (1996) 2719.
[7] N.M. Zaripov, M.V. Popik, L.V. Vilkov, T.G. Mannafov, Zh. Strukt. Khim. 21 (1980) 37.
[8] (a) H.W. Roesky, K.-L. Weber, U. Seseke, W. Pinkert, M. Noltemeyer, W. Clegg, G.M. Sheldrick, J. Chem. Soc. Dalton Trans. (1985) 565. (b) S. Vogler, W. Massa, K. Dehnicke, Z. Naturforsch Sect. B 46 (1991) 1625. (c) G. Heckmann, G. Wolmershäuser, Chem. Ber. 126 (1993) 1071. (d) M. Iwaoka, S. Tomoda, J. Org. Chem. 60 (1995) 5299.
[9] (a) M. Iwaoka, S. Tomoda, Phosphorous Sulfur Silicon Relat. Elem. 67 (1992) 125. (b) M. Iwaoka, S. Tomoda, J. Am. Chem. Soc. 118 (1996) 8077. (c) M. Iwaoka, H. Komatsu, S. Tomoda, Chem. Lett. (1998) 969. (d) H. Komatsu, M. Iwaoka, S. Tomoda, Chem. Commun. (1999) 205.
[10] F. Bigoli, P. Deplano, F.A. Devillanova, V. Lippolis, M.L. Mercuri, Eur. J. Inorg. Chem. (1998) 137.
[11] A. Jung, G. Wolmershäuser, Z. Naturforsch. 52b (1997) 345.
[12] M. Miura, Y. Takanohashi, Y. Habata, S. Akabori, J. Chem. Soc. Perkin Trans. 1 (1995) 1719.
[13] S. Hauge, K. Marøy, Acta Chem. Scand. 46 (1992) 1166.
[14] S. Bjørnevåg, P.U. Gahre, S. Hauge, O. Vikane, Acta Chem. Scand. A38 (1984) 175.
[15] U. Geiser, H.H. Wang, J.A. Schlueter, J.M. Williams, J.L. Smart, A.C. Cooper, S.K. Kumar, M. Caleca, J.D. Dudek, K.D. Carlson, J. Ren, M.-H. Whangbo, J.E. Schirber, W.R. Bayless, Inorg. Chem. 33 (1994) 5101.
[16] S. Larsen, L. Henriksen, Acta Chem. Scand. A38 (1984) 289.
[17] When diselenide **3** was reacted with an equimolar amount of Br_2 or SO_2Cl_2, the product was pure selenenyl bromide (ArSeBr) or selenenyl chloride (ArSeCl), respectively, having a strong intramolecular nonbonded Se···N interaction [9b].
[18] Selenenyl trihalides ($ArSeX_3$) are usually produced by the reaction of selenenyl halides (ArSeX) with halogens (X_2) or halogenating reagents. C. Paulmier, Selenium Reagents and Intermediates in Organic Synthesis, Pergamon Press, Oxford, 1986.
[19] According to the comprehensive search by Landrum and Hoffmann [2], similar hyperbolic structural correlation was found. However, the correlation was rather scattered because their search included for inorganic and high-coordinated selenium compounds.
[20] M.J. Frisch, G.W. Trucks, H.B. Schlegel, P.M.W. Gill, B.G. Johnson, M.A. Robb, J.R. Cheeseman, T.A. Keith, G.A. Petersson, J.A. Montgomery, K. Raghavachari, M.A. Al-Laham, V.G. Zakrzewski, A. Nanayakkara, M. Challacombe, C.Y. Peng, P.Y. Ayala, W. Chen, M.W. Wong, J.L. Andres, E.S. Replogle, R. Gomperts, R.L. Martin, D.J. Fox, J.S. Binkley, D.J. Defrees, J. Baker, J.P. Stewart, M. Head-Gordon, C. Gonzalez, J.A. Pople, Gaussian, Inc., Pittsburgh, USA, 1995.
[21] A. Schafer, H. Horn, R. Ahlrichs, J. Chem. Phys. 97 (1992) 257.
[22] A.D. Becke, J. Chem. Phys. 98 (1993) 5648.
[23] A. Altomare, G. Cascarano, C. Giacovazzo, A. Guagliardi, M.C. Burla, G. Polidori, M. Camalli, J. Appl. Crystallogr. 27 (1994) 435.
[24] G.M. Sheldrick, SHELXL-97, Program for the Refinement of Crystal Structures, University of Göttingen, Germany, 1997.
[25] L.J. Farrugia, J. Appl. Crystallogr. 30 (1997) 565.
[26] D.W. Marquardt, J. Soc. Ind. Appl. Math. 11 (1963) 431.